Hindawi Publishing Corporation
Journal of Materials
Volume 2016, Article ID 6070468, 10 pages
http://dx.doi.org/10.1155/2016/6070468

Research Article

Fabrication and Microhardness Analysis of MWCNT/MnO_2 Nanocomposite

Md. Zakir Hussain,[1] Sabah Khan,[1] Rajamani Nagarajan,[2] Urfi Khan,[3] and Vishnu Vats[4]

[1]*Department of Mechanical Engineering, Jamia Millia Islamia, New Delhi, India*
[2]*Department of Chemistry, University of Delhi, New Delhi, India*
[3]*Mechanical & Automation Engineering Department, Indira Gandhi Delhi Technical University for Women, Delhi, India*
[4]*Department of Chemistry, G. B. Pant Govt. Engineering College, New Delhi, India*

Correspondence should be addressed to Md. Zakir Hussain; mechazakirhussain@gmail.com

Received 17 April 2016; Accepted 11 August 2016

Academic Editor: Ching-Ping Wong

Recent research has shown that carbon nanotube (CNT) acts as a model reinforcement material for fabricating nanocomposites. The addition of CNT as a reinforcing material into the matrix improves the mechanical, thermal, tribological, and electrical properties. In this research paper multiwalled carbon nanotube (MWCNT), with different weight percentage (5%, 10%, and 15%), was reinforced into manganese dioxide (MnO_2) matrix using solution method. The different weight % of MWCNT/MnO_2 nanocomposite powders was compacted and then sintered. The phase analysis, morphology, and chemical composition of the nanocomposites were examined by X-ray diffractometer, Field Emission Scanning Electron Microscope (FESEM), and Energy Dispersive X-Ray (EDX), respectively. The XRD analysis indicates the formation of MWCNT/MnO_2 nanocomposites. The FESEM surface morphology analysis shows that MnO_2 nanotube is densely grown on the surface of MWCNT. Further, microhardness of MWCNT/MnO_2 nanocomposite was measured and it was found that 10 wt% has higher microhardness in comparison to 5 and 15 wt%. The microhardness of the composites is influenced by mass density, nanotube weight fraction, arrangement of tubes, and dispersion of MWCNT in H_2SO_4(aq) solution.

1. Introduction

In the last decade, nanoscience and nanotechnology have invited much interest of the researchers and industrial practitioners as enhancement in the property of the composite is noticed as the atomic dimension of reinforced material reduces to nanometer scale.

The need for advanced composite materials having enhanced functional properties and performance characteristics is ever increasing in industrial sectors. Theoretical and experimental studies have shown that CNT exhibits extremely high tensile modulus ~1 TPa and strength ~150 GPa. CNT also exhibits high flexibility, low density ~1.3–1.4 g/cm^3, and large aspect ratios ~1000 [1]. Experimental studies have also shown that MWCNT synthesized by chemical vapor deposition (CVD) exhibits Young's modulus of about 0.45 TPa and tensile strength of about 3.6 GPa during scanning electron microscope tension test [2]. The superior mechanical properties of CNT are one of the primary reasons for considering the use of CNT as a filler material for fabricating metal, ceramic, or polymer matrix nanocomposite [3].

MnO_2 is considered as an electrode material for supercapacitors because of its low cost, environmental friendly nature, nontoxicity, and excellent capacitive performance in aqueous electrolytes [4]. Many researchers have used different preparation methods of CNT/MnO_2 nanocomposites, namely, solution method, hydrothermal method, soft template method, facile synthesis method, electrodeposition method, and so forth. In comparison to simple mechanical mixing, a remarkable increase in capacitance as well as cycling performance for the nanosolution mixing of α-MnO_2

with MWCNT has been noticed [5]. Using a simple in situ hydrothermal method single crystalline MnO_2 nanoparticles were uniformly grown on the surface of MWCNT [6]. MnO_2/CNT nanocomposite was successfully synthesized by soft template method and the products had poor crystalline characteristics, and the adjacent nanorods were fused to each other irregularly to form spherical-like agglomerations and MnO_2 nanorods were absorbed on CNTs in the CNT/MnO_2 composite [7]. MWCNT/MnO_2 composite with different contents of birnessite-type MnO_2 coated on carbon nanotubes through a facile, simple, and green method of the redox reaction between $KMnO_4$ and carbon nanotubes without any other oxidant or reductant addition [8]. Using a simple hydrothermal treatment, MWCNT/MnO_2 nanocomposite with a unique nanoarchitecture was successfully synthesized [9]. The nanoporous MnO_2 sheath was composed of interconnected MnO_2 nanoflakes directly grown from the surface of the MWCNT.

A mesoporous MnO_2/CNT composite was synthesized by the reduction of $KMnO_4$ with alcohol using a soft template method and mesoporous MnO_2 was coated uniformly on the CNTs, providing a high surface area [10]. A low-cost aqueous solution method was developed to fabricate MWCNT/MnO_2 tubular nanocomposite at 80°C with interconnected MnO_2 nanoflakes coated on MWCNT [11].

Fabrication of electrodes for electrochemical supercapacitors has been done on the electrodes for electrochemical supercapacitors by cathodic electrodeposition of MnO_2 on CNTs, which were grown by CVD on stainless steel meshes [12]. A combination of simple vacuum infiltration and CVD technique was used to prepare MnO_2/CNT hybrid coaxial nanotube arrays using porous alumina templates [13]. Exceptional change of nanocomposite properties can be achieved by introducing foreign materials into the inner cylinder of carbon nanotubes and by filling of MWCNT with MnO_2 using wet chemical method [14].

With electrochemical applications already being developed for MWCNT/MnO_2 nanocomposite, continuous study of the mechanical properties of MWCNT/MnO_2 nanocomposite can lead to useful multifunctional materials with simultaneous mechanical and electrochemical applications. 10 wt% MWCNT/MnO_2 composite was prepared and investigated for its capacitance performance [5], which motivated us to find out the hardness of the nanocomposite.

The principal purpose of the hardness test is to determine the suitability of a material for a given application or the particular treatment to which the material has been subjected [15]. Microhardness is an important parameter that could be used to define the mechanical properties in relation to its microstructure. Focus has been made on the relationship of hardness with grain size for commercially pure titanium and ultrafine grained titanium [16]. Vickers and Knoop indentations of ultrafine grained titanium at different loads were ~2.5 times harder than those of pure titanium.

Indentation microhardness of the β-SiAlON ceramic using the Knoop and Vickers indenters has been measured and the results show that the measured Vickers and Knoop microindentation hardness values of the samples depend on load [17]. The variation of Vickers hardness value follows the reverse indentation size effect trend, that is, an increase in Vickers hardness value with respect to load in the low-load region beyond where it becomes relatively constant. It has been reported that the hardness of composite material depends on the nature of the material, geometry of the penetrator, and how to perform test [18]. Bulk Al-based nanocomposites with nanosized SiC by the ultrasonic cavitation-based casting method were fabricated and it was found that 2.0 wt% SiC nanoparticles achieved approximately 20% improvement of hardness [19].

2. Experimental

In this paper, we report the microhardness of 5, 10, and 15 wt% of MWCNT in MWCNT/MnO_2 nanocomposites. Also, we applied a novel technique called solution method [5] with some modification to fabricate MWCNT/MnO_2 nanocomposites powder. The solution method is simple and cost effective for preparing MWCNT/MnO_2 nanocomposite powder.

The crystallographic information of the nanocomposites was investigated by X-ray diffraction (MiniFlex 2 goniometer, X-Ray 30 kV/15 mA Div. Slit 1.25° with a scan rate of 2°/min) with a Cu K_α target. Morphologies of the MWCNT/MnO_2 nanocomposites were characterized by FESEM (Hitachi's semi-in-lens technology, model SU-70, accelerating voltage = 500 V to 30 kV, magnification: ×800,000) attached to Schottky Gun which enables dealing with EDX analysis. The sintering process was done in muffle furnace (make: Wild Barfield; model: HT25; max. temp.: 1200°C) for densification of powder particle. Also, the microhardness was measured using Vickers microhardness tester (VLPAK2000; make: Mitutoyo, Japan; model: MicroWizHard microhardness tester).

2.1. Materials and Methods

2.1.1. Materials. The reinforcing material used was MWCNT having average diameter of 20 nm, length of 50 μm, specific surface area of 60~260 m^2/gm, and 95% purity and purchased from Redox Nano Lab, Uttar Pradesh, India, and the oxidizing agent used was potassium permanganate ($KMnO_4$) of laboratory grade. The solvent used during composite preparation was sulphuric acid (2 M) solution.

2.1.2. Fabrication of MWCNT/MnO_2 Nanocomposite. The powder metallurgy route has been applied to make the pellet shape of MWCNT/MnO_2 nanocomposites. The method consists of different steps for preparation of nanocomposites and shape to products based on the heat-activated process of binding individual particles of powders.

The powder metallurgy steps are as follows.

(1) Synthesis of 5 wt% MWCNT/MnO_2 Nanocomposite. 0.10 gram of MWCNT was immersed in 250 mL of 2 M boiling H_2SO_4(aq.) and continuously stirred using magnetic stirrer for three hours, in the beaker of 500 mL capacity, to disperse MWCNT. The acid treatment in boiling H_2SO_4 results in

Figure 1: Experimental setup to prepare MWCNT/MnO_2 composite powder.

Figure 2: Die and punch assembly.

introduction of many oxygen-containing functional groups, such as carboxylic, carbonyl, and hydroxyl groups on the MWCNT surface [5]. After three hours 4 grams of $KMnO_4$ was added at 80°C–90°C. The precipitate was observed as the color of the solution changed from purple to brown. The setup is shown in Figure 1. After completion of reaction, the system was then allowed to cool down to room temperature. The obtained precipitate black in color was filtered using crucible filter and washed with deionized water and acetone to remove the remaining ions and impurities and then dried at 60°C in laboratory oven for one day. Approximately about 1.96 grams of yield was obtained.

Similarly, 10% and 15 wt% MWCNT/MnO_2 nanocomposites were synthesized. Slowly cooling down to room temperature after 3 hours of dispersion in H_2SO_4(aq) solution, the MWCNT settled down at base of beaker. This shows poor dispersion of MWCNT in the composite.

(2) Blending. The nanocomposites prepared with various weight fractions of MWCNT powders (5, 10, and 15 wt%) for uniform distribution were blended by hand blending method using mortar pestle.

(3) Compaction. The blended nanocomposites were compacted in a hydraulic press machine to produce a disc shape of solid green sample at room temperature. The pressure limiting valve was set for a maximum oil pressure of 150 kgf/cm^2. A compaction pressure of 50 kgf/cm^2 was also used to compact the test samples. The die and punch assembly used during bulk composites preparation, having maximum diameter of die of 15 mm, is shown in Figure 2.

(4) Sintering. Thermogravimetric-differential thermal analysis shows that MnO_2 decomposes rapidly to form Mn_2O_3 at temperature above 500°C [7]. Therefore sintering temperature should be below 500°C. The samples were heated up from room temperature to 450°C at a heating rate of 15°C/min for 30 minutes and this temperature was held constant for 1 hour. All samples were then allowed to attain room temperature inside the furnace before exposure to the atmosphere. The sintered samples are as shown in Figures 3(a), 3(b), and 3(c).

3. Results and Discussion

3.1. Chemical Characterization

3.1.1. X-Ray Diffraction Technique. The XRD pattern of the MWCNT shows two diffraction peaks at 26.5° and 43.2° which can be indexed as the (002) and (100) reflections of graphite, respectively, as shown in Figure 4(a) [9]. The MWCNT also contain platinum (Pt) as impurity at 2-theta value of 39.7634° having space group Fm-3m (225). In addition to the (002) and (100) diffraction peak of MWCNT, other diffraction peaks can be indexed to the tetragonal α-MnO_2 single-crystal structure and the structure of MnO_2 having space group: I4/m (87) with lattice constants of $a = 0.9815$ nm, $b = 0.9815$ nm, and $c = 0.2847$ nm used for sample refinement. 2-theta and "d" in angstrom of all major peaks for all samples are (12.964°, 6.82323), (18.209°, 4.86815), (25.68°, 3.46624), (28.769°, 3.10068), (37.605°, 2.38993), (41.988°, 2.15006), (49.89°, 1.82644), (55.997°, 1.64087), (56.787°, 1.6199), (60.02°, 1.54014), and (65.479°, 1.4243). It is confirmed that the nanorods grown on the surface of MWCNT are single-crystal α-MnO_2 [5]. The maximum peaks occur at 2-theta value of 37.605° for all samples. The XRD analysis of 10 wt% MWCNT/MnO_2 nanocomposite also shows that all the samples contain iron as impurity having space group Im-3m (229). Iron impurity may come during XRD process. The XRD patterns of 10 wt% MWCNT/MnO_2 nanocomposite are shown in Figure 4(b).

3.1.2. Surface Morphology Analysis Using Field Emission Scanning Electron Microscope (FESEM). FESEM analysis of 5 wt% MWCNT/MnO_2 composite shows that the large amount of MnO_2 nanotubes of average diameter ~25 nm is densely grown on the surface of multiwalled carbon nanotubes [5] as shown in Figure 5(a). This shows that the MnO_2 nanotubes have been synthesized using simple solution method. It can also be seen that the tubes have agglomerated which may be due to nonhomogeneous distribution of MWCNT during composite powder preparation. Similarly the surface

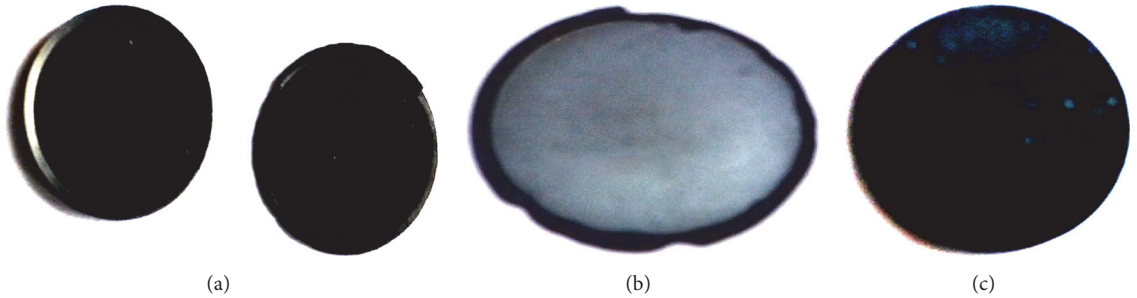

(a) (b) (c)

Figure 3: (a) 5 wt% MWCNT/MnO_2 nanocomposite. (b) 10 wt% MWCNT/MnO_2 nanocomposite. (c) 15 wt% MWCNT/MnO_2 nanocomposite.

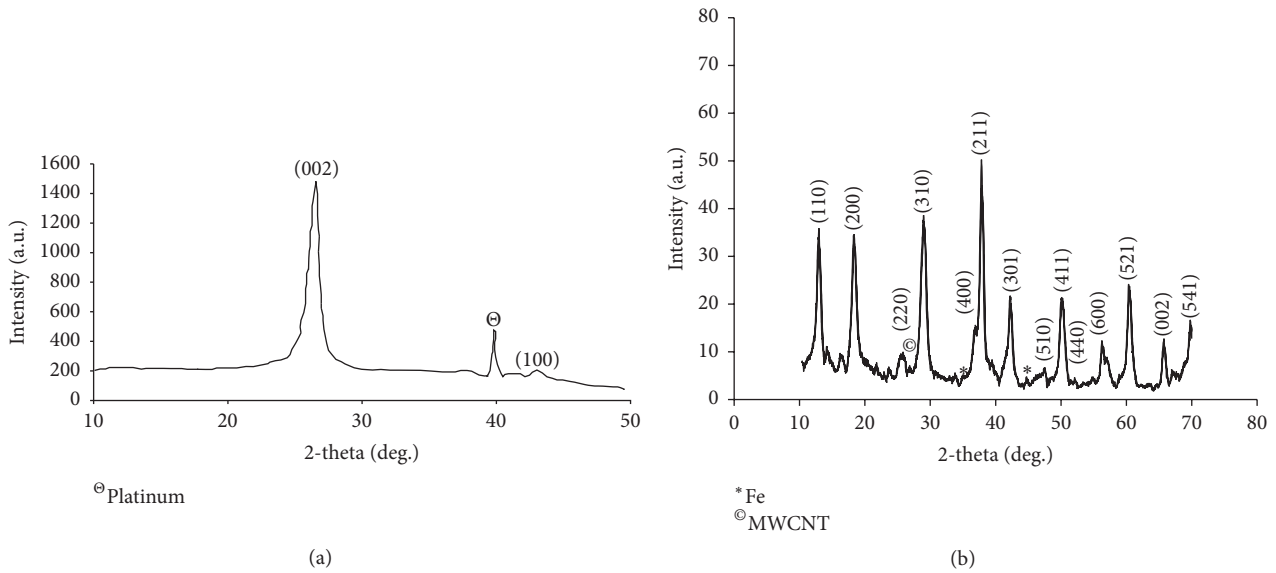

Figure 4: (a) XRD pattern of MWCNT purchased from Redex Nano Lab, Noida (UP), India. (b) XRD pattern of 10 wt% MWCNT/MnO_2 nanocomposite.

morphology analyses of 10 and 15 wt% MWCNT/MnO_2 composites show that the manganese dioxide nanotubes of average size of ~24 nm and ~22 nm range were densely grown on the surface of multiwalled carbon nanotubes as shown in Figures 5(c) and 5(e), respectively. The magnified images as shown in Figures 5(b), 5(d), and 5(f) indicate flake-like structure of MWCNT/MnO_2 nanocomposites and 10 wt% gives orderly arrangement of tubes in comparison to 5 wt% and 15 wt% of MWCNT/MnO_2 nanocomposite shows disorderly arrangement of tubes in comparison to 5 wt% and 10 wt%.

3.1.3. EDX Analysis of MWCNT/MnO_2 Composite. The spectra of the specimens were quantified to give a composition of MWCNT/MnO_2 nanocomposite. In the EDX analyses, spectrum of 5, 10, and 15 wt% MWCNT/MnO_2 nanocomposites as shown in Figures 6(a), 6(b), and 6(c) shows the presence of manganese (Mn), oxygen (O), and carbon (C). The 5 wt% MWCNT/MnO_2 nanocomposite shows the presence of impurities potassium (K), silicon (Si), and aluminium (Al). The potassium may come from $KMnO_4$ during composite powder preparation and may be located within the tunnel of α-MnO_2 [5]. Other impurities, silicon and aluminium, may come during powder metallurgy steps. The EDX analysis also indicates absence of platinum as impurity, which was found in XRD analysis of MWCNT. During nanocomposite powder preparation, the obtained precipitate black in color was filtered and washed with deionized water and acetone to remove the remaining ions and impurities which may cause removal of platinum from nanocomposite.

Table 1 shows the chemical composition of 5 wt% MWCNT/MnO_2 nanocomposite. It is found that 5 wt% contains 4.55 wt% of MWCNT.

Similarly, the 10 wt% MWCNT/MnO_2 composite also shows the presence of some impurities as sulphur (S) and potassium (K) and 15 wt% MWCNT/MnO_2 composite also contains small amount of potassium (K) as impurity.

3.1.4. Mass Density of MnO_2/MWCNT Nanocomposite. The mass density is determined using mass and volume of the nanocomposite. Table 2 shows mass density of the nanocomposite.

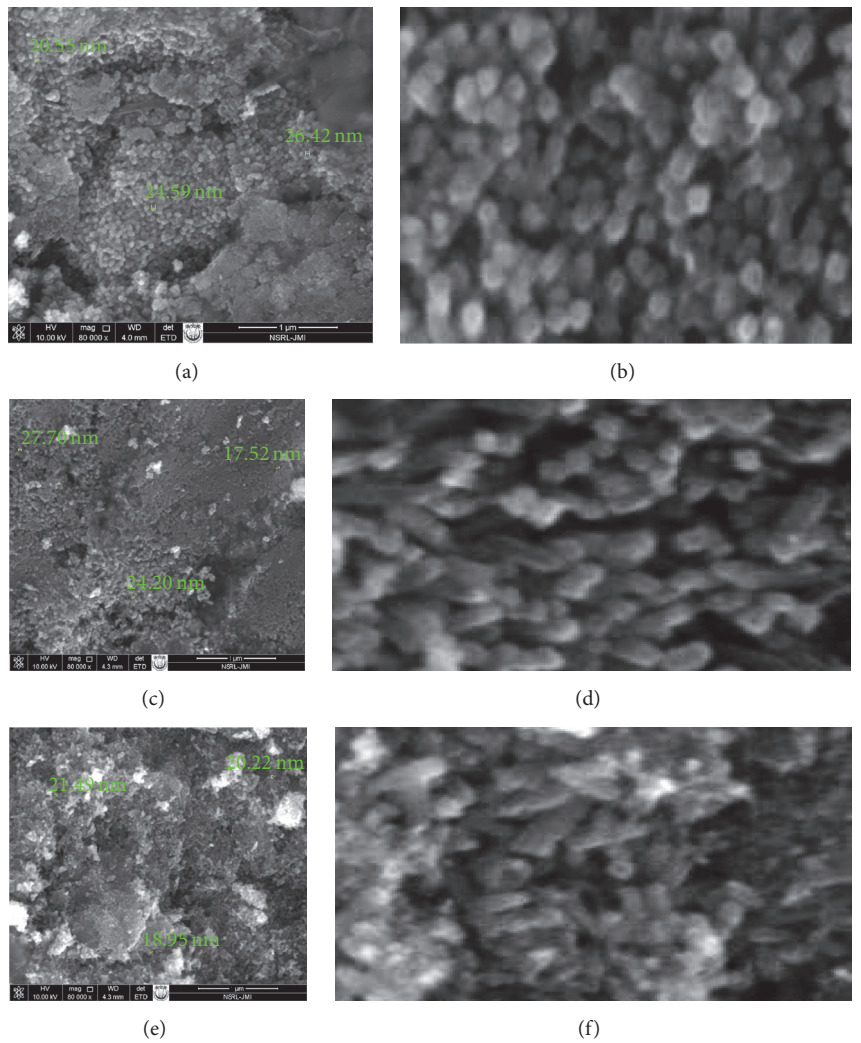

Figure 5: (a) Surface morphology of 5 wt% MWCNT/MnO_2 nanocomposite. (b) Magnified surface morphology of 5 wt% MWCNT/MnO_2 nanocomposite. (c) Surface morphology of 10 wt% MWCNT/MnO_2 nanocomposite. (d) Magnified surface morphology of 10 wt% MWCNT/MnO_2 nanocomposite. (e) Surface morphology of 15 wt% MWCNT/MnO_2 nanocomposite. (f) Magnified surface morphology of 15 wt% MWCNT/MnO_2 nanocomposite.

Table 1: Chemical composition of 5 wt% MWCNT/MnO_2 nanocomposite.

			Spectrum: 5%		
El	AN	Series	Unn. C [we%]	Norm. C [wt%]	Atom. C [at.%]
Mn	25	K-series	55.39	55.40	27.00
O	8	K-series	35.27	35.38	59.21
C	6	K-series	4.55	4.55	10.15
K	19	K-series	2.51	2.51	1.72
Si	14	K-series	0.83	0.83	0.79
Cl	17	K-series	0.52	0.52	0.39
Al	13	K-series	0.43	0.43	0.43
S	16	K-series	0.38	0.38	0.32

The density analysis shows that the density of the nanocomposite increases with addition of MWCNT from 5 wt% to 10 wt% and then decreases from 10 wt% to 15 wt% as shown in Figure 7. The 15 wt% gives less density as the FESEM analysis shows that the tubes are disorderly arranged.

Table 2: Mass density of MWCNT/MnO_2 nanocomposite.

Sl. number	Sample	Density (gm/cm^3)
1	5% MWCNT/MnO_2	2.341
2	10% MWCNT/MnO_2	2.556
3	15% MWCNT/MnO_2	2.280

3.1.5. Microhardness of MWCNT/MnO_2 Nanocomposite. Microhardness of MWCNT/MnO_2 nanocomposite was determined by microhardness tester as shown in Figure 8. The machine has minimum load of 100 gf and maximum of

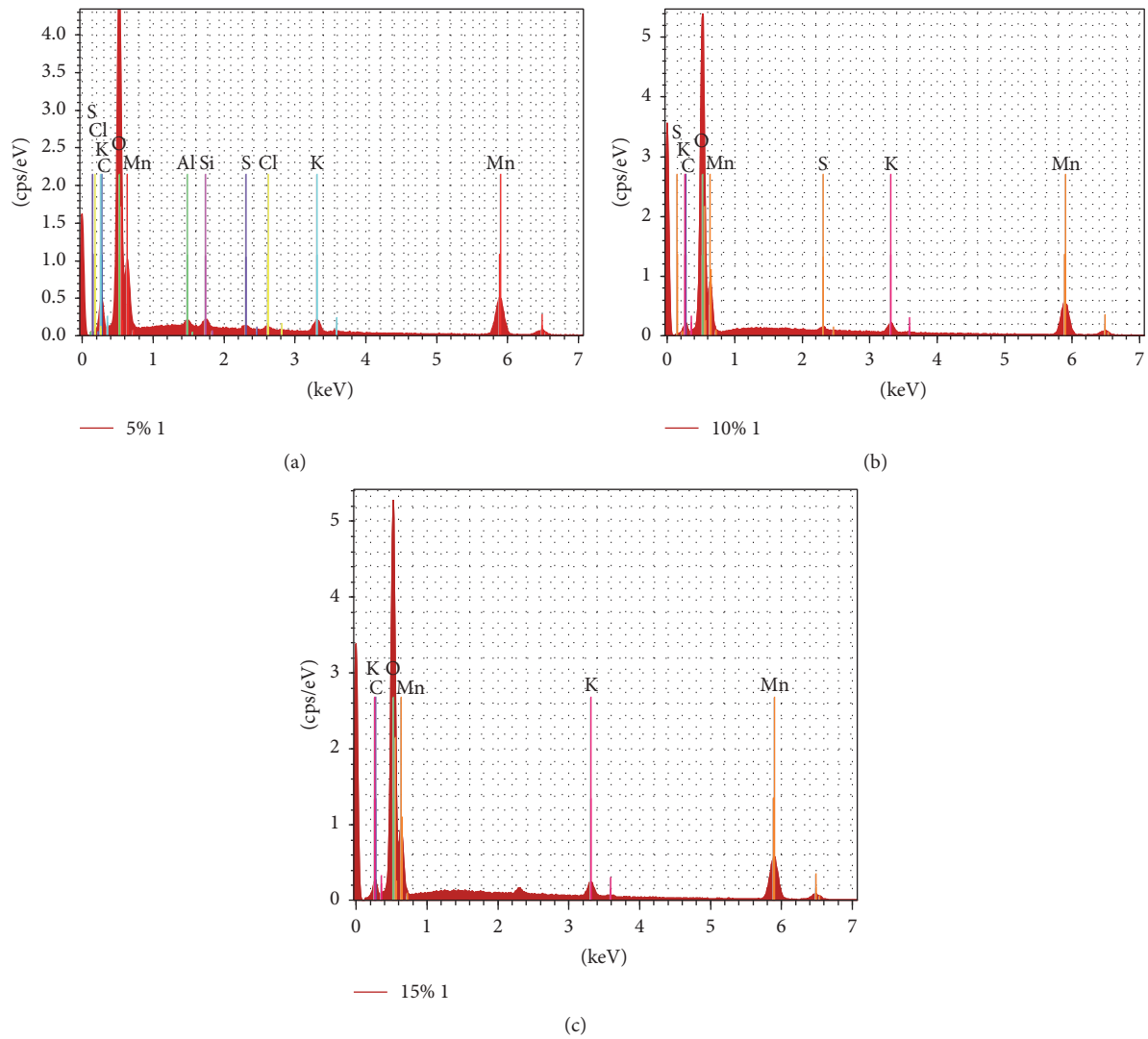

FIGURE 6: (a) Spectrum of 5 wt% MWCNT/MnO_2 nanocomposite by EDX analysis. (b) Spectrum of 10 wt% MWCNT/MnO_2 nanocomposite by EDX analysis. (c) Spectrum of 15 wt% MWCNT/MnO_2 nanocomposite by EDX analysis.

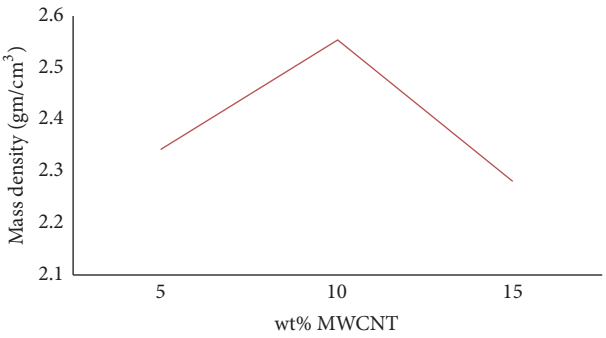

FIGURE 7: Variation of density with wt% of MWCNT.

1000 gf. Dwell time of 5–99 sec and Vickers indenter are included as shown in Figure 8. The test was carried out with 200 and 300 gf load for dwell time set at 15 seconds to ensure that the indentation is upon the surface only.

For the sample, several trials of indentation with each load were made and the average values of the diagonal lengths of indentation marks were obtained. The Vickers microhardness number H_V at each load was calculated using the following equation [15, 17]:

$$\text{Vickers hardness number } (H_V) = \frac{P \times 2\sin(136^\circ/2)}{d^2} \approx \frac{1.854P}{d^2}\ \left(\text{kgf/mm}^2\right), \quad (1)$$

where P is the applied test load in kgf, d is the average of two indentation diagonal lengths in mm, and 1.854 is a geometrical constant of the diamond pyramid.

(1) Microhardness of 5 wt% MWCNT/MnO_2 Nanocomposite. All the specimens were disc shaped of 15 mm diameter and 1.5 mm thickness. The surface finishes of nanocomposites are high and there was no need for specimen preparation

Table 3: Microhardness data of 5 wt% MWCNT/MnO_2 nanocomposite.

Observation	Applied load (P in Kgf)	d_1 (μm)	d_2 (μm)	$H_V = 1.854(P/d^2)$ (Kgf/mm^2)
1	0.2	88	83.9	50.2
2	0.2	62.9	74.1	79
3	0.2	107.9	101.7	33.7
4	0.2	117.3	106.1	29.7
5	0.2	157.2	135.6	17.3
6	0.2	157.3	142.7	16.4
7	0.2	165.7	147.7	15.1
8	0.2	134.2	118.6	23.2
9	0.2	122.3	108.5	27.8
10	0.2	134.7	126.7	21.7
11	0.2	157.4	140.6	16.7
12	0.3	201.6	185.3	14.8
13	0.3	82.2	99	67.8
14	0.3	111.8	118.6	41.9
15	0.3	193.7	176.7	16.2
16	0.3	185.2	159.6	18.7
17	0.3	211.2	193.2	13.6
18	0.3	184.6	174	17.3
19	0.3	159.3	149.7	23.3
20	0.3	169.2	154.2	21.2
21	0.3	144.6	133.8	28.7
22	0.3	267.2	238.4	8.7
23	0.3	211.2	196.2	13.4
24	0.3	168.3	152.5	21.6
Average H_V (Kgf/mm^2)				26.583

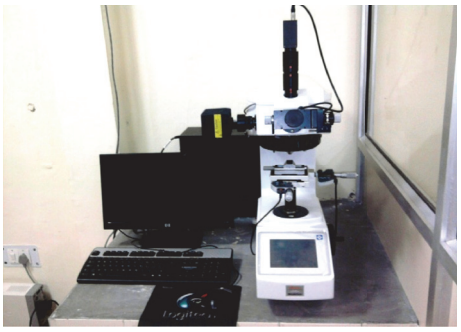

Figure 8: Microhardness tester.

for microhardness test. A total of twenty-four points on the MWCNT/MnO_2 nanocomposite and hardness at each point were measured in order to get average reading. The microhardness data of 5 wt% MWCNT/MnO_2 nanocomposite specimen is shown in Table 3. The average microhardness of 5 wt% MWCNT/MnO_2 nanocomposite is H_V = 26.583 kgf/mm^2. Some of the indentation marked by Vickers

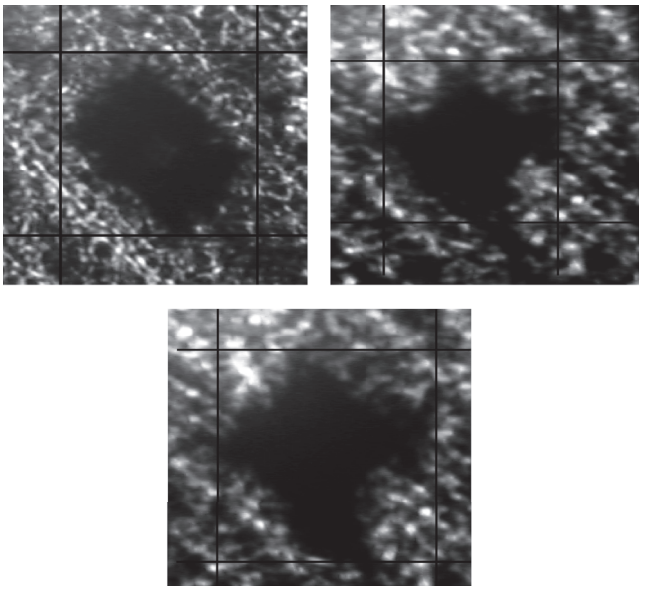

Figure 9: Surface morphograph of the indentation marked by Vickers indenter at different positions of 5 wt% MWCNT/MnO_2 nanocomposite.

Figure 10: Brittle fracture of 5 wt% MWCNT/MnO_2 nanocomposite.

indenter at different positions of 5 wt% MWCNT/MnO_2 nanocomposite is shown in Figure 9. After microhardness test, 5 wt% MWCNT/MnO_2 nanocomposite was brittle and fractured due to application of 1 kgf load as shown in Figure 10.

Similarly, the average microhardness of 10 wt% MWCNT/MnO_2 nanocomposite is H_V = 38.55 kgf/mm^2 as shown in Table 4. The indentation mark by Vickers indenter at different positions of 10 wt% MWCNT/MnO_2 nanocomposite specimen is shown in Figure 11. The 10 wt% MWCNT/MnO_2 nanocomposite was brittle and fractured due to application of load as shown in Figure 12. Similarly, the average microhardness of 15 wt% MWCNT/MnO_2 nanocomposite is H_V = 18.93 kgf/mm^2 as shown in Table 5. The indentation mark by Vickers indenter at different positions of 15 wt% MWCNT/MnO_2 nanocomposite specimen is shown in Figure 13. The 15 wt% MWCNT/MnO_2 nanocomposite

Table 4: Microhardness data of 10 wt% MWCNT/MnO_2 nanocomposite.

Observation	Applied load (P in Kgf)	d_1 (μm)	d_2 (μm)	H_V (Kgf/mm^2)
1	0.2	255.8	213.5	6.73
2	0.2	129.4	125	22.9
3	0.2	99.1	82.8	44.8
4	0.2	77.5	46.3	96.8
5	0.2	99.1	82.8	44.8
6	0.2	143.3	156.5	16.5
7	0.2	168.3	150.3	14.6
8	0.2	158.2	130.4	17.8
9	0.2	117.4	92.38	33.7
10	0.2	104.1	92.1	38.5
11	0.2	96.3	70.6	53.2
12	0.2	158.7	141.1	16.5
13	0.3	85.1	85.1	76.8
14	0.3	101.2	97.9	56.1
15	0.3	155.5	148.3	24.1
16	0.3	127.4	115.3	37.8
17	0.3	119.8	111.2	41.7
18	0.3	120.1	103.6	44.4
19	0.3	106.4	96.9	53.8
20	0.3	120.8	104.8	43.7
21	0.3	150.8	128.8	28.4
22	0.3	127.8	110.2	39.3
23	0.3	132	114.2	36.7
24	0.3	127.3	122.7	35.6
Average H_V (Kgf/mm^2)				38.55

Table 5: Microhardness data of 15 wt% MWCNT/MnO_2 nanocomposite.

Obs.	Applied load (P in Kgf)	d_1 (μm)	d_2 (μm)	H_V (Kgf/mm^2)
1	0.2	199.3	203.1	9.1
2	0.2	123.0	125.0	24.1
3	0.2	149.6	144	17.2
4	0.2	158.4	142.7	16.3
5	0.2	164.7	155.3	14.4
6	0.2	111.3	96.9	34.2
7	0.2	106.5	93.3	37.1
8	0.2	119.7	109.5	28.2
9	0.2	197.2	168.2	11.1
10	0.2	159.2	143.2	16.2
11	0.2	111.9	118.6	27.9
12	0.2	184.6	161.2	12.4
13	0.3	206.3	188.1	14.3
14	0.3	187.5	177.3	16.7
15	0.3	223.7	198.3	12.5
16	0.3	167.3	142.3	23.3
17	0.3	154.4	148.7	24.2
18	0.3	206.3	189.7	14.2
19	0.3	182.3	166.3	18.3
20	0.3	163.2	145	23.4
21	0.3	211.3	199.1	13.2
22	0.3	213.7	183.5	14.1
23	0.3	202.9	173.5	15.7
24	0.3	189.3	181.1	16.2
Average H_V (Kgf/mm^2)				18.93

was brittle and fractured as shown in Figure 14. The variation of microhardness at each position indicates nonhomogeneous distribution of MWCNT into MnO_2 matrix.

(2) Variation of Microhardness with Percentage Weight Loading of MWCNT in MWCNT/MnO_2 Nanocomposite. The variation of average microhardness with increase in weight percentage of MWCNT in MnO_2 matrix is shown in Figure 15. From the figure, it is clear that, with increase in wt% of MWCNT from 5 wt% to 10 wt%, microhardness increases from 26.583 kgf/mm^2 to 38.55 kgf/mm^2. With further addition of 15 wt% MWCNT, the microhardness value decreases to 18.93 kgf/mm^2. The increase in microhardness is attributed to increase in mass density and arrangement of tubes in MWCNT/MnO_2 nanocomposite.

4. Conclusion

In the present study, 5, 10, and 15 wt% MWCNT/MnO_2 nanocomposites were successfully synthesized by using simple solution method. From the detailed investigation of the results obtained, the following conclusions can be drawn:

(1) From the XRD patterns, tetragonal crystal structures of MnO_2 were confirmed and also the formation of MWCNT/α-MnO_2 nanocomposites was confirmed. At different wt% of MWCNT/MnO_2 nanocomposite powder, the highest peaks were observed at 2-theta of 37.605°.

(2) From surface morphology analysis by FESEM, it was confirmed that the MnO_2 nanorods were densely grown on the surface of MWCNT. The structure of MWCNT/MnO_2 nanocomposite is flake-like structure and 10 wt% gives orderly arrangement of tubes in comparison to 5 wt% and 15 wt% of MWCNT.

(3) The mass density analysis shows that the mass density of the nanocomposites increases with addition of MWCNT from 5 wt% to 10 wt% and then decreases from 10 wt% to 15 wt%.

(4) From microhardness analysis, it is clear that the addition of wt% of MWCNT into MnO_2 matrix from 5% to 10% increases the microhardness. By further addition of MWCNT up to 15%, the microhardness

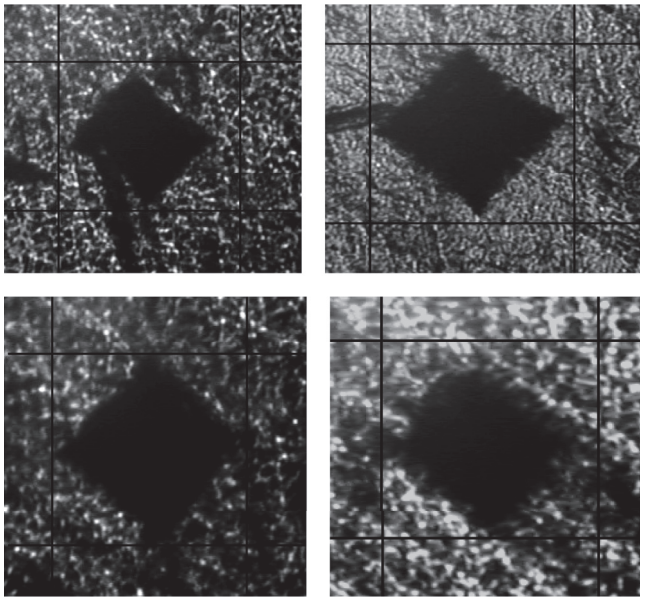

Figure 11: Surface morphograph of the indentation marked by Vickers indenter at different positions of 10 wt% MWCNT/MnO_2 nanocomposite.

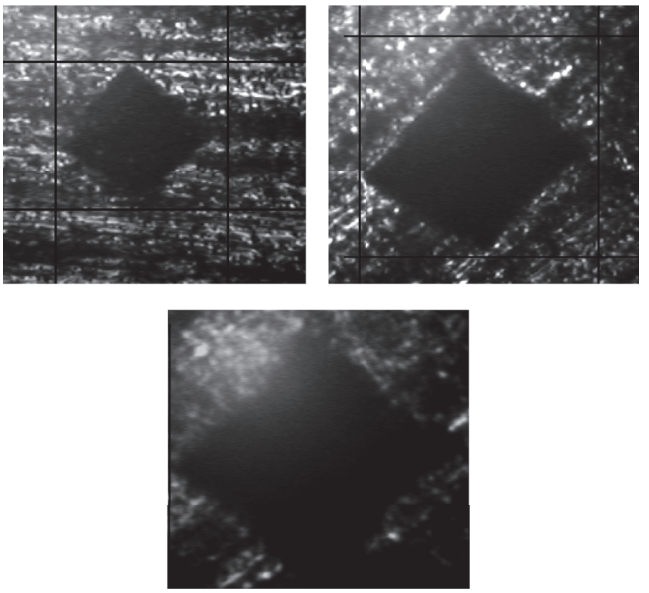

Figure 13: Surface morphograph of the indentation marked by Vickers indenter at different positions of 15 wt% MWCNT/MnO_2 nanocomposite.

Figure 12: Brittle fracture of 10 wt% MWCNT/MnO_2 nanocomposite.

Figure 14: Brittle fracture of 15 wt% MWCNT/MnO_2 nanocomposite.

decreases. The result of microhardness of these composites depends highly on their mass density; as the mass density increases, microhardness also increases.

The variation of microhardness at each position indicates nonhomogeneous distribution of MWCNT into MnO_2 matrix. All nanocomposite specimens were brittle and fractured. The adopted solution method results in poor dispersion of MWCNT as MWCNT settled at base slowly cooling to room temperature and causes lower microhardness. The structure of the nanocomposite is porous in nature [9]. The porous structure of this nanocomposite gives easy exchange of ions and increases its electrochemical property. Consequently, it decreases the mechanical properties.

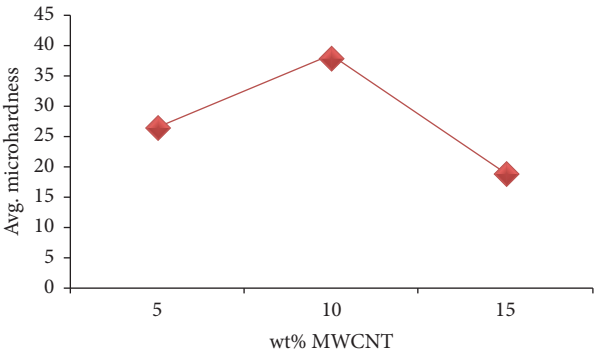

Figure 15: Variation of average microhardness with weight percentage of MWCNT.

The microhardness of the nanocomposite is influenced by density, nanotube weight fraction, arrangement of tubes, and dispersion MWCNT in H_2SO_4(aq) solution.

Competing Interests

The authors declare that they have no competing interests.

Acknowledgments

The authors are grateful for the discussions and comments by Dr. P. K. Chaudhury, Associate Professor, Department of Mechanical Engineering, Galgotia University, Noida, Uttar Pradesh, India.

References

[1] J. M. Wernik and S. A. Meguid, "Recent developments in multifunctional nanocomposites using carbon nanotubes," *Applied Mechanics Reviews*, vol. 63, no. 5, Article ID 050801, 2010.

[2] S. C. Tjong, *Carbon Nanotube Reinforced Composites*, Wiley-VCH, 2004.

[3] E. T. Thostenson, Z. Ren, and T.-W. Chou, "Advances in the science and technology of carbon nanotubes and their composites: a review," *Composites Science and Technology*, vol. 61, no. 13, pp. 1899–1912, 2001.

[4] I. Acznik, K. Lota, A. Sierczynska, and G. Lota, "Carbon-supported manganese dioxide as electrode material for asymmetric electrochemical capacitors," *International Journal of Electrochemical Science*, vol. 9, no. 5, pp. 2518–2534, 2014.

[5] Y. Chen, C. G. Liu, C. Liu, G. Q. Lu, and H. M. Cheng, "Growth of single-crystal α-MnO_2 nanorods on multi-walled carbon nanotubes," *Materials Research Bulletin*, vol. 42, no. 11, pp. 1935–1941, 2007.

[6] F. Teng, S. Santhanagopalan, and D. D. Meng, "Microstructure control of MnO_2/CNT hybrids under in-situ hydrothermal conditions," *Solid State Sciences*, vol. 12, no. 9, pp. 1677–1682, 2010.

[7] M.-M. Zou, D.-J. Ai, and K.-Y. Liu, "Template synthesis of MnO_2/CNT nanocomposite and its application in rechargeable lithium batteries," *Transactions of Nonferrous Metals Society of China*, vol. 21, no. 9, pp. 2010–2014, 2011.

[8] H. Wang, C. Peng, F. Peng, H. Yu, and J. Yang, "Facile synthesis of MnO_2/CNT nanocomposite and its electrochemical performance for supercapacitors," *Materials Science and Engineering B*, vol. 176, no. 14, pp. 1073–1078, 2011.

[9] H. Xia, Y. Wang, J. Lin, and L. Lu, "Hydrothermal synthesis of MnO_2/CNT nanocomposite with a CNT core/porous MnO_2 sheath hierarchy architecture for supercapacitors," *Nanoscale Research Letters*, vol. 7, article 33, 2012.

[10] C.-W. Lee, S.-B. Yoon, S.-M. Bak, J. Han, K. C. Roh, and K.-B. Kim, "Soft templated mesoporous manganese oxide/carbon nanotube composites via interfacial surfactant assembly," *Journal of Materials Chemistry A*, vol. 2, no. 10, pp. 3641–3647, 2014.

[11] Y.-Q. Liu, X.-W. Li, Z.-W. Wei, L.-P. Zhang, X.-C. Wei, and D.-Y. He, "Preparation and electrochemical performance of MWCNTs@MnO_2 nanocomposite for lithium ion batteries," *Science China Technological Sciences*, vol. 57, no. 6, pp. 1077–1080, 2014.

[12] Y. Wang, H. Liu, X. Sun, and I. Zhitomirsky, "Manganese dioxide-carbon nanotube nanocomposites for electrodes of electrochemical supercapacitors," *Scripta Materialia*, vol. 61, no. 11, pp. 1079–1082, 2009.

[13] A. L. M. Reddy, M. M. Shaijumon, S. R. Gowda, and P. M. Ajayan, "Coaxial MnO_2/carbon nanotube array electrodes for high-performance lithium batteries," *Nano Letters*, vol. 9, no. 3, pp. 1002–1006, 2009.

[14] S. H. S. Zein, L.-C. Yeoh, S.-P. Chai, A. R. Mohamed, and M. E. M. Mahayuddin, "Synthesis of manganese oxide/carbon nanotube nanocomposites using wet chemical method," *Journal of Materials Processing Technology*, vol. 190, no. 1–3, pp. 402–405, 2007.

[15] H. Chandler, *Hardness Testing*, ASM International, Geauga County, Ohio, USA, 2nd edition, 1999.

[16] K. P. Sanosh, A. Balakrishnan, L. Francis, and T. N. Kim, "Vickers and knoop micro-hardness behavior of coarse-and ultrafine-grained titanium," *Journal of Materials Science and Technology*, vol. 26, no. 10, pp. 904–907, 2010.

[17] H. S. Güdera, E. Şahina, O. Şahina, H. Göçmezb, C. Duranc, and H. Ali Çetinkaraa, "Vickers and knoop indentation microhardness study of β-SiAlON ceramic," *Acta Physica Polonica A*, vol. 120, no. 6, pp. 1026–1033, 2011.

[18] M. Pasăre and N. Mihuţ, "Methods for determining the properties of composite materials," *Fascicle of Management and Technological Engineering*, vol. 10, no. 20, pp. 4.118–4.123, 2011.

[19] Y. Yang, J. Lan, and X. Li, "Study on bulk aluminum matrix nano-composite fabricated by ultrasonic dispersion of nanosized SiC particles in molten aluminum alloy," *Materials Science and Engineering A*, vol. 380, no. 1, pp. 378–383, 2004.